TITLE PAGE:

Site-directed Mutagenesis of the CC Chemokine Binding Protein 35K-Fc Reveals Residues Essential for Activity and Mutations That Increase the Potency of CC Chemokine Blockade

Gemma E. White, Eileen McNeill, Ivy Christou, Keith M. Channon and David R. Greaves.

Sir William Dunn School of P athology (GEW, IC and DRG) and Department of Cardiovascular Medicine (EM and KMC) University of Oxford, Oxford, UK.

1

RUNNING TITLE PAGE:

Running title: Site-directed mutagenesis of 35K-Fc

Corresponding Author: Dr David R Greaves, Sir William Dunn School of Pathology,

University of Oxford, South Parks Road, Oxford, OX1 3RE. Tel: +441865 285519. Fax:

+441865 275515. Email: david.greaves@path.ox.ac.uk

Number of pages: 35

Number of tables: 2

Number of figures: 6

Number of references: 35

Word count of abstract: 241

Word count introduction: 771

Word count discussion: 1144

Abbreviations used in thi s manuscript: TNF; tumour necrosis factor, ECIS; electric cell substrate impedance sensing, MR; mannose receptor, LTB4; leukotriene B4.

ABSTRACT

Chemokines of the CC class are key mediators of monocyte recruitment and macrophage differentiation and have a well documented role in many inflammatory diseases. Blockade of chemokine activity is therefore an attractive target for anti-inflammatory therapy. 35K (vCCI) is a high-affinity chemokine binding protein expressed by poxviruses which binds all human and murine CC chemokines, preventing their interaction with chemokine receptors. We developed an Fc-fusion protein of 35K with a modified human IgG1 Fc domain, and expressed this construct in HEK-293T cells. Purified 35K-Fc is capable of inhibiting CC chemokine-induced calcium flux, chemotaxis and beta-arrestin recruitment in primary macrophages and transfected cells. In order to elucidate the residues involved in chemokine neutralisation, we performed site-directed mutagenesis of six key amino acids in 35K and expressed the mutant Fc-fusion proteins *in vitro*. We screened the mutants for their ability to block chemokine-induced beta-arrestin recruitment in transfected cells and to inhibit primary macrophage signalling in an electric cell substrate impedance sensing (ECIS) assay. Using a sterile model of acute inflammation, zymosan-induced peritonitis, we confirmed that wild-type 35K-Fc can reduce monocyte recruitment while one mutant (R89A) showed a more pronounced blockade of monocyte influx and another mutant (E143K) showed total loss of function. We believe that 35K-Fc will be a useful tool for exploring the role of CC chemokines in chronic inflammatory pathologies, and we have identified a higher potency form of the molecule which may have potential therapeutic applications in chronic inflammatory disease.

3

INTRODUCTION

Fc fusion proteins and monoclonal antibodies that b lock the activity of circul ating inflammatory mediators are now an essential arm of therapies directed against chronic inflammatory pathologies such as rhe umatoid arthritis (Taylor and Feldmann, 2009). One of the most successful drugs in this cla ss is the TNFR:Fc fusion protein etanercept (Enbrel), a fusion of TNFR2 with a human IgG1 Fc domain which functions as a decoy receptor for soluble TNFα (Moreland et al., 1997). The addition of an Fc domain greatly increases the half life of the TNFR protein in plasma, such that dosing is reduced to once or twice weekly injections (Moreland et al., 1996). A wide range of other soluble mediators could be targeted with this app roach, since n ot all pat ients respond to anti-TNF therapy and the efficacy of treatment may decrease over time, meaning novel targets are required (Taylor and Feldmann, 2009). One candidate class of soluble inflammatory mediators is the chemokines or chemotactic cytokines, the low molecular weight proteins responsible for the co-ordinated migration of leu kocytes in response to inflammation and infection (Charo and R ansohoff, 2006; Mackay, 2001).

Most viruses e xpress a repertoire of proteins, including chemokine binding proteins, which interfere with the host immune response as a mean s to a void rapid elimination from the organism (Alcami, 2003). Chemokines are divided into four families on the basis of structure; C, CC, CXC and CX_3C (Zlotnik and Yoshie, 2000), and viral chemokine binding proteins show differential specificity and may bind one family or multiple families. The M3 protein from murine gammaherpesvirus 68, for ex ample, binds and ina ctivates all known chemokines (Parry et al., 2000).

All poxviruses, including vaccinia virus, express a soluble 35 kDa chemokine-binding protein named '35K' or vCCI (Alcami et a l., 1998; S mith et al., 1997). 35K has no sequence homology with known proteins and the elucidation of its crystal structure showed an unusual beta-sandwich topology not seen elsewhere (Carfi et al., 1999). 35K binds all known human and mouse CC chemokines with high affinity (in the low nanomolar range) and this activity contributes directly to virulence (B urns et al., 2002; Reading et al., 2003). 35K shows the

4

highest affinity for a number of chemokines responsible for monocyte/macrophage recruitment including MCP-1 (CCL2), MIP-1α (CCL3), MIP-1β (CCL4) and RANTES (CCL5), and indeed b inds these chemokines with a higher aff inity than th ey bind their cognate receptors (Burns et al., 2002). A solution structure of 35K in complex with the chemokine MIP-1β (CCL4) demonstrated that 35K binds tightly across the face o f the c hemokine, obscuring regions essential for chemokine receptor binding (Zhang et al., 2006). This study, and others which generated mutant CC chemokines, identified key residues involved in the 35K-chemokine interaction (Beck et al., 2001; Zhang et al., 2006). The critical residues in MCP-1 required for high affinity binding to 35K were identified as Arg18, Tyr13, and Arg24 – the same residues required for inte raction with the M CP-1 receptor CCR2 (Beck et al., 2001). Thus, 35K may bind to chemokines in solution or bound onto t he cell surface by glycosaminoglycans, thereby preventing the adhesion and directed migration of cells expressing the appropriate chemokine receptors.

35K has been shown to reduce eosinophil infiltration in a guinea pig skin model of allergic inflammation and decreased airway inflammation in a model of allergic asthma (Alcami et al., 1998; Dabbagh et al., 2000). Both these models are dominated by eotaxin induced inflammatory cell recruitment, a ch emokine which has moderate to low affinity for 35 K compared to other CC chemokines. The highest affinity ligands for 35K are the inflammatory chemokines known to recruit monocytes in chronic inflammatory pathologies including rheumatoid arthritis and atherosclerosis (Burns et al., 2002). Indeed, our laboratories have shown that viral delivery of 35K suppresses both diet-induced and vein graft atherosclerosis in Apoe^{-/-} mice (Ali et al., 2005; Bursill et al., 2004; Bursill et al., 2008).

Viral delivery of 35K is not ideal for several reasons including the inflammatory response generated by the virus, the d ifficulty in administering a known dose and the short ter m duration of expression in the case of adenovirus (Nayak and Herzog, 2010). We therefore generated a 35 K-Fc fusion protein of vaccinia virus 35K with the modified Fc dom ain of human IgG1. In order to identify amino acid residues essential for 35K activity, we performed site-directed mutagenesis of 35K-Fc and tested mutants for their ability to block chemokine

effects on p rimary and t ransfected cells and in a murine model of sterile peritonitis. Importantly, we generated a num ber of loss-of funct ion mutants with single amino acid substitutions and identified a residue within 35K, which when mutated, leads to enhanced blockade of CC chemokine activity *in vitro* and *in vivo.*

MATERIALS AND METHODS

Materials

All cell culture media and buffers w ere obtained from PAA systems (Yeovil, UK) unless otherwise specified. All laboratory chemicals were from S igma-Aldrich (Gillingham, UK) unless otherwise specified. PCR primers were from Eurofins MWG Biotech (London, UK), PCR reagents were from Qiagen (C rawley, UK). Chemokines were purchased from Peprotech (London, UK).

Cloning and mutagenesis of 35K-Fc

DNA encoding 35K from vaccinia virus (Lister str ain) including the endogenous signal peptide was amplified from a ve ctor containing the entire 35K gene u sing the fo llowing primers F-GCATGCTAGCATGAAACAATATATCGTC R-GCCGGAATTCGACACACGCTTTGAGTTT encoding a 5' N heI site and a 3' E coRI site using the HotStar Taq P CR kit from Qiagen according to m anufacturer's instructions. 35K was cloned in frame and upstream of a human IgG1 Fc domain using the pSecTag2(C) vector (Invitrogen, Paisley, UK). The Fc portion had been previously mutated to contain the substitutions L234A, L235E and G 237A to abrogate Fc receptor binding and P 331S to prevent complement activation. 35K-Fc was mutated using the S tratagene QuikChange mutagenesis kit (Agilent Technologies, Stockport, UK) according to m anufacturer's instructions, and mutants screened by sequencing in both directions. The primers used for mutagenesis are listed in Table 1. The MR-Fc construct described here is a non- functional mutant of the cysteine-rich domain of the mannose receptor fused to the same mutated IgG1 Fc (Taylor et al., 2004) and was a kind gift from Dr Philip Taylor (Department of Infection, Immunity and Biochemistry, Cardiff University).

Production of 35K-Fc protein

7

Plasmid DNA was prepared using the Endofree Plasmid maxi kit (Invitrogen, Paisley, UK) and transfected into 293T cells in triple layer T175 flask s (Nunc, Rochester, NY) using Genejuice transfection reagent (M erck, Nottingham, UK) according to manufacturer's instructions. 24 hours post-transfection, cells were transferred to serum-free media (DMEM + 0.1% w/v BSA) and protein expression continued for 5 days. Conditioned media containing 35K-Fc was concentrated using a Vivaflow 50 tangential flow machine with a 30 kDa filter (Generon, Maidenhead, UK), then applied to a P roteus protein A midi column (Pierce, Cramlington, UK). Bound protein was washed 2x with PBS/0.01% Tween-20 then eluted with 0.5 M sodium citrate pH3 followed by neutralisation with 1.5 M Tris-HCl pH10. Eluted protein was dialysed 2x overnight against 4L PBS, then re-concentrated using a centrifugal concentrator with a 30 kDa cut-off (Generon, Maidenhead, UK). Protein yield was assessed using a NanoDrop spectrophotometer at 280nm, protein integrity was assessed on an SDS-PAGE gel, and endotoxin testing was performed using the Pyrogene recombinant factor C assay (Lonza, Slough, UK).

Bio-gel elicitation of primary mouse macrophages

All animal studies were conducted with ethical approval from the Dunn School of Pathology Local Ethical Review Committee and in accordance with the UK Home Office regulations (Guidance on the O peration of Animals, Scientific Procedures Act, 1986). C57Bl6/J or SV129 mice (Harlan, UK) were injected intra-peritoneally (i.p.) with 1 ml of 2% Bio-gel P-100 fine polyacrylamide beads (45-90 µm; Bio-rad laboratories, Hemel Hempstead, UK) suspended in PBS and 4 days later, mice were sacrificed and the peritoneum lavaged with 10 ml ice-cold PBS / 2 m M EDTA (for chemotaxis and xCELLigence assays). Room temperature PBS / EDTA was used for lavage of cells for calcium flux assays.

Calcium flux

Cells (1×10^7/ml) were loaded with Fura-PE3 AM calcium sensitive dye (Merck, Nottingham, UK) at a concentration of 1.5 µM in calcium flux buffer (HBSS / 5 mM HEPES / 0.5% w/v

8

BSA) for 45 mins at room temperature with gentle agitation. Cells were washed twice with calcium flux buffer then resuspended at a concentration of 3×10^7 cells/ml. Calcium flux was assessed using a Perkin Elmer LS55 spectrofluorimeter in a cuvette containing 100 µl of cells and 300 µl buffer. Agonists were added in a volume of 10 µl at a concentration of 40x. When 35K-Fc was used, agonists were pre-incubated with 35K-Fc for 2 hours at room temperature prior to assay.

Chemotaxis

Chemotaxis was assessed using Neuroprobe ChemoTx 96 well plates (Receptor Technologies, Leamington Spa, UK) as described previously (Cash et al., 2008). Agonists were pre-incubated with 35K-Fc for 2 hours at room temperature and loaded into the lower well of the plate. Bio-gel elicited primary mouse macrophages were resuspended at 5×10^6 cells/ml in chemotaxis buffer (RPMI / 25 mM HEPES / 0.5% w/v BSA) and 80 µl of cell suspension (4×10^5 cells) was placed on top of a filter with an 8 µm pore size. Cells were allowed to migrate for 4 hours, then unmigrated cells on top of the filter were removed by wiping with cotton buds. Migrated cells on the underside were fixed with 1% v/v formalin for 10 mins, then stained with DAPI for 5 mins and filters mounted onto slides. Migrated cells were assessed by fluorescence microscopy and quantified using MetaMorph software. Data are expressed as migration index, i.e. fold change over the response to media alone.

DiscoveRx PathHunter eXpress beta arrestin assay

The assay was performed according to manufacturer's instructions (DiscoveRx Corp., Birmingham, UK). Briefly, cells were thawed and plated in OCC media in half area 96 well luminescence plates (white walled, clear bottom) and allowed to recover for 48 hours. Agonists were-preincubated +/- 35K-Fc for 2 hours at room temperature and then added to the cells for 90 minutes at 37 °C. Detection reagents were added and incubated with the cells for 90 mins at room temperature. Luminescence was measured using a 96 well plate luminometer (Berthold instruments, Harpenden UK) and WinGlow Software.

9

Roche xCELLigence ECIS assay

Experiments were performed using a 96 w ell xCELLigence SP instrument (Roche Diagnostics, Burgess Hill, UK). Bio-gel elicited macrophages were plated at 200,000 cells/well in 96 w ell xCELLigence plates i n OptiMEM media (Invitrogen, Paisley UK) and allowed to adhere for 6 hours before the media was changed to remove non-adherent cells. The following day agonists were pre-incubated +/- 35K-Fc for 2 hours at room temperature and then added to the cells and data collected every 2 seconds. T he data were normalised to addition o f media alone and then the maximum cell index (i.e. peak height) was calculated. Experiments using CCR2 transfected CHO cells were performed with 25000 cells per well.

Zymosan Induced Peritonitis

Zymosan-induced peritonitis was performed as described previously (Cash et al., 2009). Briefly, C57Bl6/J mice (Harlan, UK) were injected i.p. with 10 µg zymosan A (Sigma-Aldrich, Gillingham UK) diluted in 0.5 ml PBS or vehicle alone. Two hours later, mice w ere injected with 15 µg 35K-Fc in 0.5 ml PBS or v ehicle alone. After a further tw o hours, mice were sacrificed and the peritoneal cavity was lavaged with 5ml PBS / 2mM EDTA. Peritoneal cell counts were performed using a haemocytometer and trypan blue exclusion and peritoneal exudate cells were stained with antibodies against Ly6G (BD Biosciences, Oxford, UK) and 7/4 (AbD Serotec, Kidlington, UK) and analysed by flow cytometry to assess neutrophi l and inflammatory monocyte recruitment (see supplementary figure 1 for representative primary data). Cell-free peritoneal lavage fluid was stored at -80 °C for later ELISA analysis.

35K sandwich ELISA

Maxisorb ELISA plates (Nunc, Rochester NY) were coated overnight at room temperature with vCCI (35K) capture antibody (R&D systems) at 1 µg/ml in PBS. Plates were washed 5x with dH$_2$O then non-specific binding was blocked with blocking buffer (PBS / 0.25% BSA /

1mM EDTA) for 2 hours at room temperature. Lavage samples (undiluted) or standards were incubated on the plate for 2 hours, washed off, then incubated with anti-human Fc HRP antibody (1:5000, Jackson ImmunoResearch). The plate was incubated with substrate (Sigma Fast OPD) then the reaction stopped with 3M H_2SO_4. Calculated concentrations were multiplied by the lavage volume (5 ml) to obtain total µg 35K-Fc per peritoneal cavity.

JE sandwich ELISA

Peritoneal lavage samples were assayed for JE (mouse CCL2/MCP-1) concentration using a Duoset sandwich ELISA (R&D systems, Abingdon, UK) according to manufacturer's instructions. Samples were assayed undiluted. Calculated concentrations were multiplied by the lavage volume (5 ml) to obtain total ng JE per peritoneal cavity.

11

RESULTS

35K-Fc specifically blocks CC chemokine induced calcium flux and chemotaxis

Purified 35K-Fc protein w as tested for its ability to block CC chemokine signalling in a calcium flux assay with stably transfected 300.19 murine B cells. 300.19 CCR2 cells showed a robust calcium flux in response to the CC chemokine MCP-1 (CCL2), but failed to respond to the CX_3C chemokine fractalkine (FK / CX_3CL1; Figure 1A). Similarly, 300.19 CX_3CR1 cells responded to fractal kine, but showed no response to M CP-1 (Figure 1 B). Both cell lines responded to SDF-1α (CXCL12) via their endogenous CXCR4 receptor (Figure 1A and B). MCP-1 pre-incubated w ith 35K-Fc failed to induce a c alcium flux in 300.19 CCR2, and a second addition of MCP-1 also failed to induce signalling – presumably due to rapid binding and inactivation of the chemokine by 35K-Fc (Figure 1C). SDF-1α still induced a calcium signal, indicating a specific blockade of CC chemokine signalling (Figure 1C). Furthermore, 35K-Fc had no effect on the response to the CX_3C chemokine fractalkine in 300.19 CX_3CR1 cells (Figure 1D). A second addition of fractalkine failed to induce a cal cium flux response, presumably due to homologous desensitisation of the CX_3CR1 receptor (Figure 1D).

To further confirm the specificity of the CC chemokine blockade by 35K-Fc, we performed a calcium flux assay in primary Bio-gel elicited murine macrophages. These cells showed a robust calcium flux response to the CC chemokine agonist MIP-1α (CCL3) and the non-chemokine GPCR agonist leukotriene B4 (LTB4) which acts through the BLT1 receptor (data not shown). 35K-Fc almost completely abrogated the response to MIP-1α, but had no effect on the response to LTB4 (Figure 2A). A second addition of MIP-1α alone did elicit a calcium flux showing the cells were capable of re sponding. A control Fc protein (MR-Fc: a non-functional fusion of the cysteine rich domain of mannose receptor w ith the same IgG1 Fc domain (Taylor et al., 2004)) had no effect on the macrophage response to MIP-1α, indicating the blockade is specific to 35K-Fc (Figure 2B). A second addition of MIP-1α failed to induce a significant calcium flux presumably due to homologous desensitisation of the receptor.

12

We next tested whether 35K-Fc could inhibit chemotaxis of primary macrophages towards CC chemokines. Bio-gel elicited murine macrophages were allowed to migrate towards increasing concentrations of MIP-1α and showed a bell-shaped dose response curve, which is typical in this modified Boyden chamber assay (Figure 2C). We then chose a fixed dose of 0.5 nM MIP-1α, and pre-incubated the chemokine with increasing doses of 35K-Fc for 1 hour prior to addition to the assay. 35K-Fc induced a dose dependent blockade of MIP-1α-induced migration which was statistically significant at doses of 5, 10 and 20 nM (Figure 2D). 35K-Fc had no effect on macrophage chemotaxis towards the potent chemoattractant chemerin (a non-chemokine) at any dose tested (data not shown).

Site directed mutagenesis and screening by PathHunter eXpress beta-arrestin GPCR assay

Site directed mutagenesis of MCP-1, a high affinity ligand for 35K, indicated that the residues Y13, R18 and R24 in the chemokine were essential for binding to both 35K and the MCP-1 receptor, CCR2 (Beck et al., 2001). These residues are highly conserved among all CC chemokines, and a solution structure of MIP-1β bound to rabbitpox 35K indicated that these same residues were closely contacted by 35K and highlighted the critical residues involved (Zhang et al., 2006). We targeted a number of residues within 35K based on the information provided by the co-structure. D141 and E143 interact closely with the positively charged R18 residue in the chemokine, we therefore generated charge-swap mutants D141R, E143K and E143R and alanine mutants D141A and E143A, as well as a D141L mutant with a larger, hydrophobic, uncharged side chain. Phe13 in the chemokine was shown to contact a cluster of hydrophobic residues including V185 and Y217. We generated alanine mutants at these two residues, and also generated a polar Y217N mutant in order to disrupt the hydrophobic binding site. Finally, mutagenesis of MCP-1 by Beck *et al.* revealed that the mutation K49A in MCP-1 increased its affinity for 35K by 3 fold, possibly by relieving steric hindrance in this region of interaction (Beck et al., 2001). In the co-structure, this residue was found to be closely contacted by the residues Y80 and R89 in 35K (Zhang et al.,

13

2006). We hypothesised that alanine mutants of these residues in 35K would show higher affinity chemokine binding than the WT protein.

Mutant 35K-Fc proteins were produced in exactly the same way as WT protein and integrity assessed by SDS-PAGE gel and western blotting with anti-35K antibody (data not shown). In order to screen the mutants for their effect on CC chemokine activity, we utilised a rapid and robust GPCR signalling assay based on β-arrestin recruitment in transfected cell lines (DiscoveRx PathHunter eXpress).

RANTES induced a dose-dependent activation of CCR5 with an EC_{50} of 2nM (Figure 3A). To test the effect of 35K-Fc on CCR5 activation by RANTES, 5nM RANTES (the EC_{80} in this assay) was pre-incubated for 2 hours with 35K-Fc at a range of concentrations then added to the assay. WT 35K-Fc inhibited CCR5 activation and beta-arrestin recruitment with an IC_{50} of 5.6 nM (Figure 3B). MR-Fc had no effect on CCR5 activation by RANTES at any dose tested (Figure 3B).

To screen the mutants, 5 nM RANTES was pre-incubated with 35K-Fc at a fixed dose (15 nM) for 2 hours then added to the assay. When RANTES was pre-incubated with WT 35K-Fc, the response was approximately 38% of that with RANTES alone (Figure 3C). All other mutants, except V185A, had a significantly different effect (p<0.001) on RANTES signalling at CCR5 compared to WT 35K-Fc. Mutations at D 141 and E 143 significantly inhibited chemokine blockade, with the E143K and E143R charge-swap mutants showing complete (>95%) loss of function, indicating the crucial importance of contact with the Arg18 residue in the chemokine (Figure 3C). Mutations targeting the interaction with Phe13 in the chemokine indicated that the V185 residue in 35K is not critically involved in the interaction, while Y217 mutation does reduce the extent of chemokine blockade but this residue is not essential for function (Figure 3C).

We hypothesised that the two mutants Y80A and R89A would show an increased ability to block chemokine signalling. In fact, the Y80A mutant showed complete loss of functi on indicating that this residue is e ssential for contact with K49 in the chemokine. In contrast, R89A showed an enhanced blockade of RANTES signalling compared to W T 35K-Fc

(p<0.001), reducing the response to 18% compared to RANTES alone (Figure 3C). The control protein, MR-Fc was completely unable to block RANTES signalling, showing the specificity of the CC chemokine blockade (Figure 3C). We also screened selected mutants in a second signalling assay (xCELLigence) using CCR2 transfected cells which measures the effect of chemokines on electric cell-substrate impedance sensing (see below). Data for all mutants is summarised in Table 2.

R89A is a more potent inhibitor of *in vitro* chemokine activity than WT 35K-Fc

We chose to take two mutants for further analysis *in vitro*, the loss-of-function mutant E143K and the R89A mutant with enhanced inhibitory activity. In a CCR2 beta-arrestin assay, WT 35K-Fc inhibited the response to MCP-1 with an IC_{50} of 12.9 nM in the experiment shown, while R89A 35K-Fc was significantly more potent (p<0.001) and inhibited MCP-1 signalling with an IC_{50} of 2.8 nM (Figure 4B, pooled data from independent experiments is shown in Table 2). In a CCR5 beta-arrestin assay, WT 35K-Fc inhibited the response to RANTES with an IC_{50} of 7.2 nM in the experiment shown, while R89A 35K-Fc was again more potent (p<0.05) and inhibited RANTES signalling with an IC_{50} of 2.5 nM (Figure 4D, pooled data from independent experiments is shown in Table 2). R89A also showed a more potent blockade of the CCR7 ligand MIP-3β (CCL19; p<0.01; Table 2). In contrast, E143K 35K-Fc had no effect on either MCP-1 or RANTES induced receptor activation, indicating it is a loss-of-function mutant (Figure 4B and D, Table 2). Neither WT nor R89A 35K-Fc were able to block the activity of IL-8 (CXCL8) on the CXCR2 receptor, indicating a specific blockade of CC chemokine activity only (Figure 4F).

To test whether the mutants showed similar activity on primary cell responses to chemokines, we utilised an electric cell-substrate impedance sensing (ECIS) assay (Roche xCELLigence) which measures changes in cell impedance as a result of functional responses (Yu et al., 2005). Primary Bio-gel elicited primary murine macrophages were plated in a 96 well xCELLigence plate, where the base of the plate is covered with gold electrodes. Alternating current is passed through the cell monolayer every 2 seconds and

15

impedance measured in an arbitrary unit termed 'cell index'. When cells are stimulated with an agonist, a change in impedance occurs which causes an increase in the cell index which can be measured over time. Representative primary data obtained by treating macrophages with either MIP-1α (CCL3) or SDF-1α (CXCL12) is shown in figure 5A and 5B respectively.

The chemokine MIP-1α (CCL3) induced a dose-dependent increase in cell index in primary murine macrophages with an EC_{50} of approximately 0.9 nM (Figure 5A and 5C). To test the effect of the 35K-Fc mutants on this response, 4 nM MIP-1α (~EC_{80} of the assay) was pre-incubated with increasing concentrations of WT or mutant 35K-Fc for 2 hours then applied to the assay. WT 35K-Fc inhibited the response to MIP-1α with an IC_{50} of 3.6 nM in the experiment shown (Figure 5E, pooled data from independent experiments is shown in Table 2). R89A 35K-Fc was approximately twice as potent as WT 35K-Fc ($p<0.05$), and inhibited the response with an IC_{50} of 1.7 nM in the experiment shown (Figure 5E, pooled data from independent experiments is shown in Table 2). E143K was completely unable to inhibit the response to MIP-1α (Figure 5E). To confirm that R89A 35K-Fc remained a specific inhibitor of CC chemokines, we used the CXC chemokine SDF-1α in the same assay. In primary murine macrophages, SDF-1α induced an increase in cell index with an EC_{50} of approximately 4.7 nM (Figure 5B and 5D). Neither WT nor R89A 35K-Fc had any effect on the response when pre-incubated with SDF-1α prior to addition to the assay (Figure 5F).

R89A shows enhanced blockade of monocyte recruitment *in vivo* compared to WT 35K-Fc

In order to test the effect of wild-type and mutant 35K-Fc on inflammatory cell recruitment *in vivo*, we utilised a sterile model of peritonitis induced by the yeast cell wall component zymosan (Cash et al., 2009). To determine whether 35K-Fc could inhibit ongoing inflammation, mice were injected intraperitoneally with zymosan, then 2 hours later were injected with wild-type or mutant 35K-Fc. A low dose of 35K-Fc was chosen (15 µg) such that potential differences in activity between mutants could be quantified. Peritoneal lavage was carried out 2 hours later (after 4 hours overall) and total cell counts were performed as

16

well as staining and flow cytometry to measure neutrophil and monocyte recruitment (see supplementary figure 1 for representative FACS data). WT 35K-Fc (15 µg) significantly reduced monocyte recruitment by 30% (Figure 6A; p<0.05) but had no effect on neutrophil influx (Figure 6B) or total cell numbers in the cavity (data not shown). The R89A mutant also significantly blocked monocyte recruitment into the cavity by 43% (Figure 6A; p<0.001), while the E143K mutant showed total loss of function and had no effect on monocyte recruitment (Figure 6A).

We also assessed the level of the CC chemokine JE (mouse MCP-1/CCL2) in peritoneal lavage fluid from the same animals using an ELISA capable of detecting free chemokine and that bound to 35K-Fc protein. Control mice receiving vehicle alone (PBS, PBS group) had a low level of peritoneal JE (0.13 ng/cavity; Figure 6C) and this increased 3.5-fold to 0.49 ng/cavity following the injection of zymosan (ZY, PBS group; Figure 6C). Injection of 35K-Fc protein alone also led to an increase in the level of peritoneal JE detectable (0.63 ng/cavity; PBS, 35K group). Mice receiving zymosan followed by WT 35K-Fc (ZY, WT group) had significantly more peritoneal JE than mice receiving zymosan alone (0.78 ng/cavity; p<0.05, Figure 6C). Furthermore, injection of zymosan followed by R89A 35K-Fc further enhanced the level of detectable JE (1.1 ng.cavity; p<0.001), while injection of the loss-of-function E143K mutant did not significantly alter the level of peritoneal JE compared to animals receiving zymosan alone (0.34 ng/cavity; Figure 6C).

To confirm that all animals received equivalent doses of the 35K-Fc proteins, we assayed the lavage fluid with a 35K sandwich ELISA. Two hours post-injection, there was approximately 1 µg 35K-Fc remaining in the peritoneal cavity and no significant difference between treatment groups (Figure 6D).

DISCUSSION

Using site-directed mutagenesis, this study has identified residues in a 35K-Fc fusion protein which are essential for CC chemokine binding, those which are dispensable, and others which can be mutated to enhance chemokine blockade. Following the generation of a 35K-Fc fusion protein, we have shown specific and potent blockade of CC chemokine activity *in vitro* and demonstrated anti-inflammatory activity *in vivo*. Based on the published co-structure between 35K and MIP-1β (Zhang et al., 2006), we produced a series of mutants targeting key residues and tested their function *in vitro*. With the substitution of a single residue – E143K, we generated a 35K-Fc protein that is incapable of blocking CC chemokine activity *in vitro* and *in vivo* and we identified a residue (R89) which when mutated to alanine, leads to a 35K-Fc protein with increased potency of CC chemokine blockade and enhanced anti-inflammatory activity.

The solution co-structure between 35K and MIP-1β, showed several key regions at the interface between 35K and the chemokine (Zhang et al., 2006). These included the acidic residues D141 and E143 and the hydrophobic pocket including the residues V185 and Y217. We have demonstrated that E143 is the only essential residue for the electrostatic interaction with R18 on the chemokine, since the charge swap mutants E143K and E143R show complete loss of activity. D141 mutations impair the function of 35K but do not result in total loss of function. Mutation of residues in the hydrophobic pocket involved in contacting F13 in the chemokine, revealed that the V185 residue in 35K is not required, while Y217 is important but not essential for the interaction. Finally, experiments by Beck *et al*. indicated that mutation of K49 in MCP-1 increased the interaction with 35K (Beck et al., 2001). We hypothesised that mutation of the interacting residues on 35K (Y80 and R89) would increase the potency of CC chemokine blockade. In fact, Y80 was shown to be essential since mutation to alanine completely abrogated the function of 35K-Fc. However, the R89A mutant showed a 3-4 fold higher chemokine blocking activity compared to WT 35K-Fc.

In a murine model of sterile peritonitis, 35K-Fc was able to significantly reduce monocyte but not neutrophil recruitment at a relatively low dose (15 µg). The lack of effect of neutrophil

18

recruitment is not unexpected, since the recruitment of neutrophils in this model is driven by multiple factors including CXC chemokines and complement components e.g. C5a. The dose used in this study is in line with clinically used Fc fusion proteins since 15 μg per mouse equates to a dose of 750 μg/kg which in a 70 kg adult would equate to a 50 mg injection – the recommended weekly dose for the anti-TNF Fc fusion protein etanercept. Our results also compare favourably with another study reporting the use of 35K-Fc in an air-pouch model of inflammation induced by carrageenan (Buatois et al., 2010) The authors demonstrated a 50% reduction in macrophage recruitment after 72 hours following a 6 hour pre-treatment with 200 μg vCCi (35K)-Fc. This is approximately 13 times the dose used in our study. Furthermore, our data show we can inhibit an ongoing inflammation induced by zymosan, a situation more relevant to inflammatory disease.

In this study we found that although WT and R89A 35K-Fc were able to significantly reduce monocyte infiltration into the peritoneal cavity, the apparent level of the monocyte chemoattractant JE was increased. This is in line with previous studies from our laboratory which showed that adenoviral delivery of 35K increased the plasma level of the CC chemokines RANTES and MIP-1α while reducing the bioactivity of these chemokines (Bursill et al., 2003). We interpret this finding as evidence that 35K-Fc is able to bind and sequester chemokines in solution, preventing both their activity and clearance. Thus, the higher potency R89A mutant showed the most striking inhibition of monocyte recruitment, but conversely induced the largest increase in detectable JE levels, while the E143K mutant neither reduced monocyte recruitment nor affected the peritoneal JE level compared to zymosan alone. This is consistent with two possible hypotheses. Firstly, since the binding sites for 35K and GAGs (glyocsaminoglycans) on chemokines are independent and differ in affinity by up to 1000 fold (35K having a low nM affinity, and GAGs an approximate μM affinity (Burns et al., 2002; Lau et al., 2004)), 35K-Fc may 'strip' chemokines bound to GAGs on the cell surface, thus increasing their apparent concentration in solution while disrupting chemokine gradients known to be essential for migration *in vivo* (Proudfoot et al., 2003). Secondly, binding to 35K-Fc may prevent the normal routes of chemokine clearance and

degradation via decoy receptors such as D6 expressed on both lymphatic endothelial cells and recruited leukocytes (Colditz et al., 2007; Graham and McKimmie, 2006; Weber et al., 2004). D6 knockout mice show an excessive response to inflammatory stimuli and in a cutaneous inflammation model these mice fail to clear inflammatory chemokines in the resolution phase of inflammation, demonstrating a critical role for this receptor in chemokine clearance and degradation (Jamieson et al., 2005). Despite the fact that 35K-Fc may interfere with pathways of chemokine clearance, our results have demonstrated that 35K-Fc retains anti-inflammatory activity *in vivo,* suggesting chemokines must remain bound and inactive. The pathways by which 35K-bound chemokines are cleared and degraded remain to be elucidated.

Fc fusion proteins and monoclonal antibodies that inhibit the activity of inflammatory mediators including TNFα and IL-1β are now an established therapeutic strategy in many chronic inflammatory diseases. However, not all patients respond successfully to the currently available treatment options. Chemokines may provide a novel target for therapeutic blockade in inflammatory diseases including rheumatoid arthritis, inflammatory bowel disease and atherosclerosis where mouse models have shown an essential role for chemokines in pathogenesis (Boring et al., 1998; Braunersreuther et al., 2007). However, targeting a single chemokine or chemokine receptor may not prove successful since the chemokine network shows a significant level of redundancy: most chemokines bind 'promiscuously' to more than one chemokine receptor and many key chemokine receptors have multiple high affinity chemokine ligands. Indeed a recent study targeting a single chemokine receptor (CCR2) in atherosclerosis with a small molecule antagonist could not halt plaque progression in experimental animals (Olzinski et al., 2010). In comparison, our laboratories have previously shown that both adenoviral and longer term lentiviral delivery of 35K is sufficient to reduce both macrophage content and plaque size in a mouse model of atherosclerosis (Bursill et al., 2004; Bursill et al., 2008).

In this study we have generated a series of novel 35K-Fc fusion proteins which identify the key residues involved in CC chemokine blockade. Furthermore, we have generated a mutant

20

protein (R89A 35K-Fc) which is more potent than the wild-type protein. These proteins should be a useful research tool to study the role of CC chemokines in pathogenesis. We believe 35K-Fc may find therapeutic application in broad-spectrum blockade of circulating chemokines in chronic inflammatory diseases.

21

ACKNOWLEDGEMENTS

22

AUTHORSHIP CONTRIBUTIONS

Participated in research design: White, McNeill, Christou, Channon, Greaves.

Conducted experiments: White, Greaves.

Contributed new reagents or analytic tools: McNeill.

Performed data analysis: White

Wrote or contributed to the writing of the manuscript: White, Greaves.

REFERENCES

Alcami A (2003) V iral mimicry of cytokines, chemokines and the ir receptors. *Nat Rev Immunol* **3**(1):36-50.

Alcami A, Symons JA, Collins PD, Williams TJ and Smith GL (1998) Blockade of chemokine activity by a soluble che mokine binding protein from vaccinia virus. *J Immunol* **160**(2):624-633.

Ali ZA, Bursill CA, Hu Y, Choudhury RP, Xu Q, Greaves DR and Channon KM (2005) Gene Transfer of a Broad Spectrum CC-Chemokine Inhibitor Reduces Vein Graft Atherosclerosis in Apolipoprotein E-Knockout Mice. *Circulation* **112**(9_suppl):I-235-241.

Beck CG, Studer C, Zuber JF, Demange BJ, Manning U and Urfer R (2001) The viral CC chemokine-binding protein vCCI inhibits monocyte chemoattractant protein-1 activity by masking its CCR2B-binding site. *J Biol Chem* **276**(46):43270-43276.

Boring L, Gosling J, Cleary M and Charo IF (1998) Decreased lesion formation in CCR2-/-mice reveals a role for chemokines in the initiation of at herosclerosis. *Nature* **394**(6696):894-897.

Braunersreuther V, Zernecke A, Arnaud C, Liehn E A, Steffens S, Shagdarsuren E, Bidzhekov K, Burger F, Pelli G, Luckow B, Mach F and Weber C (2007) Ccr5 But Not Ccr1 Deficiency Reduces Development of Diet-Induced Atherosclerosis in Mice. *Arterioscler Thromb Vasc Biol* **27**(2):373-379.

Buatois V, Fagete S, Magistrelli G, Chatel L, Fischer N, Kosco-Vilbois MH and Ferlin WG (2010) Pan-CC Chemokine Neutralization Restricts Splenocyte Egress and Reduces Inflammation in a Model of Arthritis. *The Journal of Immunology* **185**(4):2544-2554.

Burns JM, Dairaghi DJ, Deitz M, Tsang M and Schall TJ (2002) Comprehensive mapping of poxvirus vCCI chemokine-binding protein. Expanded range of ligand interactions and unusual dissociation kinetics. *J Biol Chem* **277**(4):2785-2789.

Bursill CA, Cai S, Channon KM and Greaves DR (2003) Adenoviral-mediated delivery of a viral chemokine binding protein blocks CC-chemokine activity in vitro and in vivo. *Immunobiology* **207**(3):187-196.

Bursill CA, Choudhury RP, Ali Z, Greaves DR and Channon KM (2004) Broad-spectrum CC-chemokine blockade by gene tra nsfer inhibits macrophage recruitment and atherosclerotic plaque formation in apolipoprotein E-knockout mice. *Circulation* **110**(16):2460-2466.

Bursill CA, McNeill E, Wang L, Hibbitt OC, Wade-Martins R, Paterson DJ, Greaves DR and Channon KM (2008) Lentiviral gene transfer to reduce atherosclerosis progression by long-term CC-chemokine inhibition. *Gene Ther* **16**(1):93-102.

Carfi A, Smith CA, Smolak PJ, McGrew J and W iley DC (1999) Structure of a sol uble secreted chemokine inhibitor vCCI (p35) from cowpox virus. *Proc Natl Acad Sci U S A* **96**(22):12379-12383.

Cash JL, Hart R, Russ A, Dixon JP, Colledge WH, Doran J, Hendrick AG, Carlton MB and Greaves DR (2008) Synthetic chemerin-derived peptides suppress inflammation through ChemR23. *J Exp Med* **205**(4):767-775.

Cash JL, White GE and Greaves DR (2009) Chapter 17. Zymosan-induced peritonitis as a simple experimental system for the study of inflammation. *Methods Enzymol* **461**:379-396.

Charo IF and Ransohoff RM (2006) The many roles of chemokines and chemokine receptors in inflammation. *N Engl J Med* **354**(6):610-621.

Colditz IG, Schneider MA, Pruenster M and Rot A (2007) Chemokines at large: in-viv o mechanisms of their transport, presentation and c learance. *Thromb Haemost* **97**(5):688-693.

Dabbagh K, Xiao Y, Smith C, Stepick-Biek P, Kim SG, Lamm WJ, Liggitt DH and Lewis DB (2000) Local blockade of al lergic airway hyperreactivity and infl ammation by the poxvirus-derived pan-CC-chemokine inhibitor vCCI. *J Immunol* **165**(6):3418-3422.

25

Graham GJ and McKimmie CS (2006) Chemokine scavenging by D6: a movable feast? *Trends in Immunology* **27**(8):381-386.

Jamieson T, Cook DN, Nibbs RJB, Rot A, Nixon C, McLean P, Alcami A, Lira SA, Wiekowski M and Graham GJ (2005) The chemokine receptor D6 limits the inflammatory response in vivo. *Nat Immunol* **6**(4):403-411.

Lau EK, Paavola CD, Johnson Z, Gaudry J-P, Geretti E, Borlat Fdr, Kungl AJ, Proudfoot AE and Handel TM (2004) Identification of the Glycosaminoglycan Binding Site of the CC Chemokine, MCP-1. *Journal of Biological Chemistry* **279**(21):22294-22305.

Mackay CR (2001) Chemokines: immunology's high impact factors. *Nat Immunol* **2**(2):95-101.

Moreland LW, Baumgartner SW, Schiff MH, Tindall EA, Fleischmann RM, Weaver AL, Ettlinger RE, Cohen S, Koopman WJ, Mohler K, Widmer MB and Blosch CM (1997) Treatment of Rheumatoid Arthritis with a Recombinant Human Tumor Necrosis Factor Receptor (p75)-Fc Fusion Protein. *N Engl J Med* **337**(3):141-147.

Moreland LW, Margolies G, Heck LW, Jr., Saway A, Blosch C, Hanna R and Koopman WJ (1996) Recombinant soluble tumor necrosis factor receptor (p80) fusion protein: toxicity and dose finding trial in refractory rheumatoid arthritis. *J Rheumatol* **23**(11):1849-1855.

Nayak S and Herzog RW (2010) Progress and prospects: immune responses to viral vectors. *Gene Ther* **17**(3):295-304.

Olzinski AR, Turner GH, Bernard RE, Karr H, Cornejo CA, Aravindhan K, Hoang B, Ringenberg MA, Qin P, Goodman KB, Willette RN, Macphee CH, Jucker BM, Sehon CA and Gough PJ (2010) Pharmacological inhibition of C-C chemokine receptor 2 decreases macrophage infiltration in the aortic root of the human C-C chemokine receptor 2/apolipoprotein E-/- mouse: magnetic resonance imaging assessment. *Arterioscler Thromb Vasc Biol* **30**(2):253-259.

Parry CM, Simas JP, Smith VP, Stewart CA, Minson AC, Efstathiou S and Alcami A (2000) A Broad Spectrum Secreted Chemokine Binding Protein Encoded by a Herpesvirus. *J Exp Med* **191**(3):573-578.

Proudfoot AE, Handel TM, Johnson Z, Lau EK, LiWang P, Clark-Lewis I, Borlat F, Wells TN and Kosco-Vilbois MH (2003) Glycosaminoglycan binding and oli gomerization are essential for the in vivo activity of certain chemokines. *Proc Natl Acad Sci U S A* **100**(4):1885-1890.

Reading PC, Symons JA and Smith GL (2003) A soluble chemokine-binding protein from vaccinia virus reduces virus virulence and the inflammatory response to infection. *J Immunol* **170**(3):1435-1442.

Smith CA, Smith TD, Smolak PJ, Friend D, Hagen H, Gerhart M, Park L, P ickup DJ, Torrance D, Mohler K, Schooley K and Goodwin RG (1997) Poxvirus genomes encode a secreted, soluble protein that preferentially inhibits beta chemokine activity yet lacks sequence homology to k nown chemokine receptors. *Virology* **236**(2):316-327.

Taylor PC and F eldmann M (2009) Anti-TNF biologic agents: still the therapy of choice for rheumatoid arthritis. *Nat Rev Rheumatol* **5**(10):578-582.

Taylor PR, Zamze S, Stillion RJ, Wong SY, Gordon S and Martinez-Pomares L (2004) Development of a specific system for targeting protein to metallophilic macrophages. *Proc Natl Acad Sci U S A* **101**(7):1963-1968.

Weber M, Blair E, Simpson CV, O'Hara M, Blackburn PE, Rot A, Graham GJ and Nibbs RJB (2004) The C hemokine Receptor D6 Constitutively Traffics to and fro m the Cell Surface to Internalize and Degrade Chemokines. *Mol Biol Cell* **15**(5):2492-2508.

Yu N, Atienza JM, Bernard J, B lanc S, Zhu J, Wang X, Xu X and A bassi YA (2005) Real-Time Monitoring of Morphological Changes in Living Cells by Electronic Cell Sensor Arrays: An Approach To S tudy G Protein-Coupled Receptors. *Analytical Chemistry* **78**(1):35-43.

Zhang L, Derider M, McCornack MA, Jao SC, Isern N, Ness T, Moyer R and LiWang PJ

(2006) Solution structure of the complex between poxvirus-encoded CC chemokine

inhibitor vCCI and human MIP-1beta. *Proc Natl Acad Sci U S A* **103**(38):13985-

13990.

Zlotnik A and Yoshie O (2000) Chemokines: a new classification system and their role in

immunity. *Immunity* **12**(2):121-127.

28

FOOTNOTES

29

FIGURE LEGENDS

Figure 1: *35K-Fc inhibition of chemokine-induced calcium flux in transfected cells.* 300.19 cells stably transfected with CCR2 or C X$_3$CR1 were loaded w ith the r atiometric calcium sensitive dye Fura-PE3 AM and analysed using a spectrofluorimeter. Chemokines (2.5 nM) were added at the indi cated timepoints and data collected every 0.5 seconds (A and B). Chemokines (2.5 nM) were pre-incubated with 50 nM 35K-Fc for 2 hours at room temperature prior to addition (C and D). Panels A-D are representative of three independent experiments, each with two technical replicates per experiment.

Figure 2: *35K-Fc inhibition of chemokine-induced calcium flux and chemotaxis in primary mouse macrophages.* A and B: Bio-gel elicited murine macrophages from SV129 mice were loaded with the ratio metric calcium sensitive dye Fura-PE3 AM and analysed using a spectrofluorimeter. MIP-1α (10 nM) and LTB4 (1 μM) were added at the indicated times and data collected every 0.5 seconds (A and B). MIP-1α was pre-incubated with 30 nM 35K-Fc (A) or MR-Fc (B) for 2 hours prior to addition. Data are representative of three independent experiments, with two technical replicates per experiment. C and D: Bio-gel-elicited murine macrophages from SV129 mice in the upper chamber of a Neuroprobe ChemoTx plate were allowed to migrate towards the indicated concentration of MIP-1α for 4 hours (C). Migration was assessed by staining cells on the underside of the chemotaxis filter. Data shown as migration index i.e. fold change over media alone and are t he mean + SEM of 4- 6 independent experiments, each w ith 3 technica l replicates per e xperiment. (D) Primary macrophages were allowed to migrate for 4 hours towards MIP-1α (0.5 nM) which had been pre-incubated with the indicated concentration of 35K-Fc for 30 mins. Data shown as % of 0.5 nM MIP-1α-induced migration, and are the mean + SEM of 4 independent experiments, with three technical replicates per ex periment. Statistical analysis performed by one-way ANOVA and D unnett's multiple comparison post te st. *p<0.05 relative to MI P-1α alone, ***p<0.001 relative to media alone (C) or MIP-1α alone (D).

Figure 3: *Screening of 35K-Fc mutants by CCR5 DiscoveRx assay.* (A) Dose-response curve showing recruitment of beta-arrestin in response to CCR5 activation by RANTES as measured by PathHunter eXpress assay (DiscoveRx). (B) RANTES (5nM) was pr e-incubated for 2 hours with the indicated concentration of WT 35K-Fc (closed circles) or MR-Fc (open circl es) then added to the assay. Panels A and B show mean + SEM of two technical replicates and are re presentative of 3 independent experiments. (C) RANTES (5nM) was pre-incubated with the indicated 35K-Fc mutant (fixed dose 15nM) then added to PathHunter eXpress CCR5 transfected cells and beta-arrestin recruitment measured according to manufacturer's instructions. Data are shown as % of the response to RANTES alone and are the mean of two independent experiments + SEM, each w ith two technical replicates for tw o batches of protei n (i.e. 4 wells per mutant per experiment). Statistical analysis performed by one-way ANOVA and D unnett's multiple comparison post test. ***p<0.001 relative to WT 35K-Fc.

Figure 4*: Comparison of 35K-Fc WT, R89A and E143K proteins by DiscoveRx beta arrestin assay.* (A) Dose-response curve of beta arrestin recruitment in response to CCR2 activation by MCP-1. (B) MCP-1 (3nM) was pre-incubated with the indicated concentration of WT 35K-Fc (closed circles), R89A 35K-Fc (squares) or E143K 35K-Fc (open circles) for 2 hours then applied to the DiscoveRx assay. (C and D) As for parts (A) and (B) using CCR5 DiscoveRx cells and RANTES as the chemokine ligand. (E and F) As for parts (A) and (B) using CXCR2 DiscoveRx cells and IL-8 as the chemokine ligand. A and B show the mean + SEM of two technical replicates and are representative of 2-3 independent experiments. C and D show the mean + SEM of tw o technical replicates and are repr esentative of 3-4 independent experiments. E and F show the mean + SEM of two technical re plicates and are representative of 2 independent experiments.

Figure 5: *Comparison of 35K-Fc WT, R89A and E143K proteins by x CELLigence assay in primary murine macrophages.* Bio-gel-elicited peritoneal murine macrophages were plated in a 96 well ECIS plate (Roche xCELLigence) overnight and allowed to adhere. The next day, cells were treated with the indicated concentration of MIP-1α (A and C), or SDF-1α (B and D). Traces were normalised to wells which received vehicle alone (Optimem medium) and the cell index was measured at 2 second intervals for 45 mins (primary data shown for MIP-1α (A) and SDF-1α (B)). To obtain dose response curves, the maximum cell index (i.e. peak height) over the 45 min timecourse was calculated (C and D). WT (closed circles), R89A (squares) or E143K (open circles) 35K-Fc was pre-incubated with 4nM MIP-1α (E) or SDF-1α (F) for 2 hours then applied to the assay and maximum cell index calculated as for B and D. Panels C to F show a single technical replicate representative of t hree independent experiments each performed with two separate batches of each mutant protein.

Figure 6: *Comparison of 35K-Fc WT, R89A and E143K in a mouse model of zymosan-induced peritonitis.* Mice were injected i.p. with Zymosan (ZY, 10 µg) or vehicle alone (PBS). Two hours later mice were injected i.p. with 15 µg of the indicated 35K-Fc protein or vehicle (PBS). After a further two hours, mice were sacrificed, the peritoneal cavity was lavaged and total cell counts were performed alongside FACS analysis for Ly 6G and 7/4 to identify inflammatory monocytes (A) and neutrophils (B) (see supple mentary figure 1 for representative primary data). (C) Peritoneal lavage samples were assayed with a JE ELISA against a recombinant protein s tandard curve. Data shown as ng JE / cavity. (D) Lavage samples were assayed with a 35K -Fc sandwich ELISA and the c oncentration estimated against a reco mbinant protein stan dard curve. Data shown as µ g 35K-Fc / cavity. Two independent experiments were performed with each mutant 35K-Fc protein, bars represent mean + SEM of 6-10 animals per group. Statistical analysis performed by one-way ANOVA and Dunnett's multiple comparison post test, ***$p<0.001$, *$p<0.05$ compared to z ymosan, PBS group.

TABLES

Table 1: Sequences of primers used for site-directed mutagenesis of 35K-Fc

| Mutation	Forward primer	Reverse primer
Y80A	TGTAGATCCTCCTACCACTGCTTACTCCATCATCGGTGGA	TCCACCGATGATGGAGTAAGCAGTGGTAGGAGGATCTACA
R89A	CATCATCGGTGGAGGTCTGGCAATGAACTTTGGATTCACC	GGTGAATCCAAAGTTCATTGCCAGACCTCCACCGATGATC
D141A	CTCTTGCTATGATCAAAGCCTGTGAGGTGTCTATCGA	TCGATAGACACCTCACAGGCTTTGATCATAGCAAGAG
D141L	GTGAAGAAGCTCTTGCTATGATCAAACTCTGTGAGGTGTCTATC	GATAGACACCTCACAGAGTTTGATCATAGCAAGAGCTTCTTCAC
D141R	GTGAAGAAGCTCTTGCTATGATCAAACGCTGTGAGGTGTCTATC	GATAGACACCTCACAGCGTTTGATCATAGCAAGAGCTTCTTCAC
E143A	CTATGATCAAAGACTGTGCGGTGTCTATCGACATCAG	CTGATGTCGATAGACACCGCACAGTCTTTGATCATAG
E143K	AGCTCTTGCTATGATCAAAGACTGTAAGGTGTCTATCGA	TCGATAGACACCTTACAGTCTTTGATCATAGCAAGAGCT
E143R	GAAGCTCTTGCTATGATCAAAGACTGTAGGGTGTCTATCGACA	TGTCGATAGACACCCTACAGTCTTTGATCATAGCAAGAGCTTC
V185A	CATCGGTTCAACGATCGCCGATACAAAATGCGTCA	TGACGCATTTTGTATCGGCGATCGTTGAACCGATG
Y217A	AGGTCAAGGATGGATTCAAGGCTGTCGACGGATCGGC	GCCGATCCGTCGACAGCCTTGAATCCATCCTTGACCT
Y217N	CAAGGATGGATTCAAGAATGTCGACGGATCGGC	GCCGATCCGTCGACATTCTTGAATCCATCCTTG

33

Table 2: Summary of data for 35K-Fc mutants

| Mutant	% RANTES response (CCR5 DiscoveRx)	IC$_{50}$ (nM) in CHO-CCR2 xCelligence	IC$_{50}$ (nM) in CCR5 DiscoveRx	IC$_{50}$ (nM) in CCR2 DiscoveRx	IC$_{50}$ (nM) in CCR7 DiscoveRx	IC$_{50}$ (nM) in MΦ xCelligence	Overall Rank
WT	35.1	90.0	**6.6** ± 0.9 (3)	**13.9** ± 1 (3)	**12.2** ± 0.4 (2)	**3** ± 0.8 (3)	3
Y80A	95.6	>1000	-	-	-	-	10
R89A	15.1	20.6	**3.7** ± 1.7 (4) *	**3.1** ± 0.4 (2) ***	**4.1** ± 0.1 (2) **	**1** ± 0.4 (3) *	1
D141A	74.3	139.0	-	-	-	-	4
D141L	80.6	>750	-	-	-	-	8
D141R	79.4	>700	-	-	-	-	=6
E143A	71.7	-	-	-	-	-	5
E143K	93.9	>5000	UD (3)	UD (2)	-	UD (3)	=11
E143R	92.5	-	-	-	-	-	=11
V185A	26.5	50.0	-	-	-	-	2
Y217A	66.5	>5000	-	-	-	-	7
Y217N	67.5	>1400	-	-	-	-	=6
MR-Fc	91.2	>1400	UD (3)	UD (2)	-	UD (3)	9

Column 2 summarises data shown in figure 3C and indicates the % of the response to 5 nM RANTES (set as 100%) in a CCR5 DiscoveRx assay following pre-incubation of 5 nM RANTES with 15 nM 35K-Fc. Column 3 gives the IC$_{50}$ in nM (mean of two technical replicates) for the indicated 35K-Fc mutant in a single xCELLigence ECIS screening assay with CCR2 transfected CHO cells responding to 10 nM MCP-1. Columns 4 to 7 show the mean IC$_{50}$ +/- SD from the number of independent experiments as indicated in brackets. Statistical analysis was performed by unpaired t test, *p<0.05, **p<0.01, ***p<0.001 relative to WT 35K-Fc treatment. Columns 4 and 5 summarise the data shown in figure 4, column 7 summarises the data shown in figure 5. Column 6 gives the IC$_{50}$ in nM for the indicated 35K-Fc mutant in a DiscoveRx assay with CCR7 transfected CHO cells responding to 10 nM MIP-3β (CCL19). UD indicates the IC$_{50}$ could not be determined i.e. a curve could not be

fitted. The final column indicates th e overall rank of the m utants where 1 = most potent
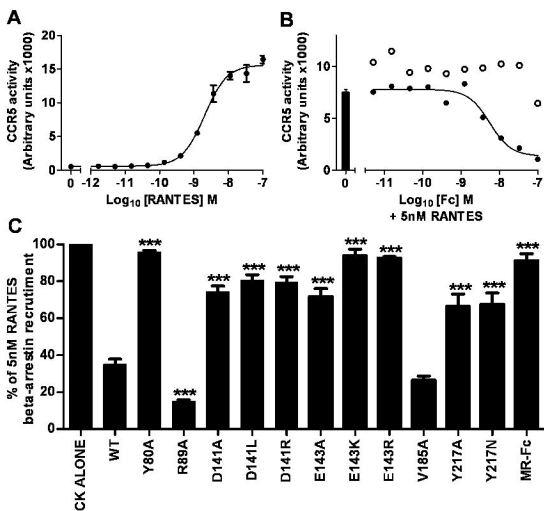
chemokine blockade and 11 = least potent.
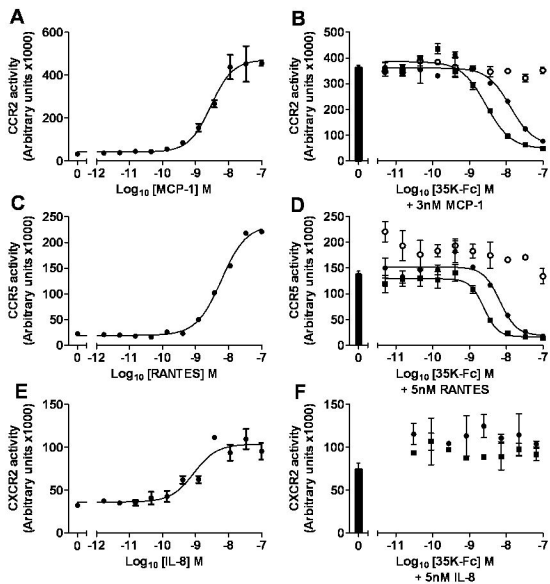
35
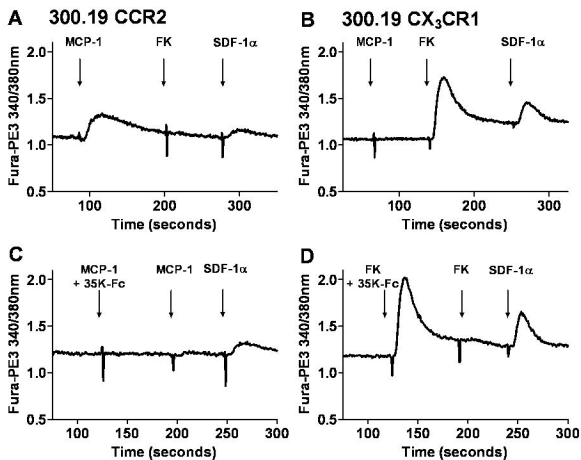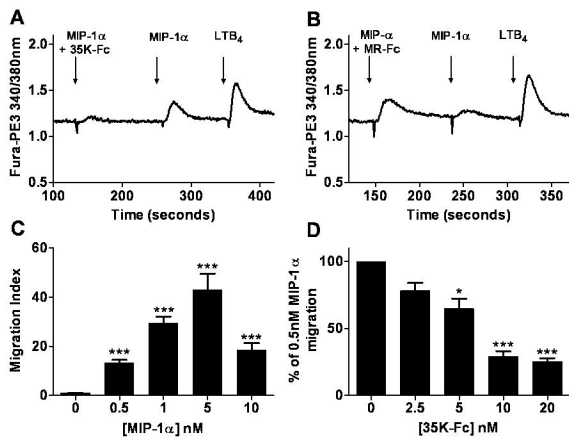
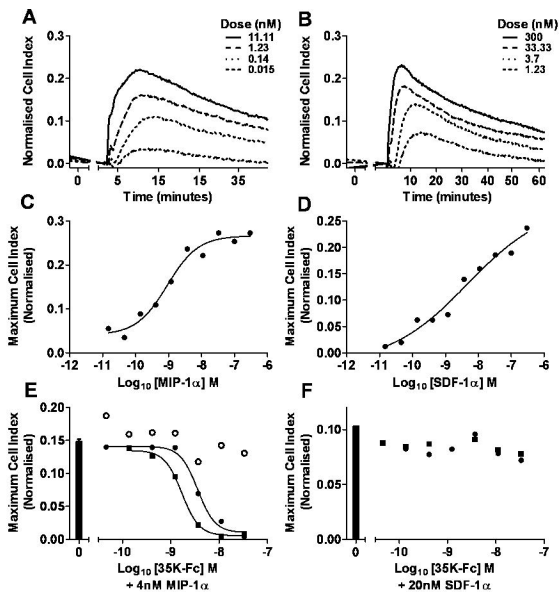# Figure 1

Figure 2

Figure 3

Figure 4

Figure 5

Figure 6